ACS APPLIED MATERIALS & INTERFACES

Research Article

www.acsami.org

"Yin and Yang" Tuned Fluorescence Sensing Behavior of Branched 1,4-Bis(phenylethynyl)benzene

Xiaohuan Sun, Yanyu Qi, Huijing Liu, Junxia Peng, Kaiqiang Liu, and Yu Fang*

Key Laboratory of Applied Surface and Colloid Chemistry, Ministry of Education, School of Chemistry and Chemical Engineering, Shaanxi Normal University, Xi'an 710062, P. R. China

Supporting Information

ABSTRACT: Achieving high sensing performance and good photostability of fluorescent films based on adlayer construction represents a significant challenge in the area of functional fluorescent film research. A solution may be offered by "Yin and Yang", a balance idea from Chinese philosophy, for the design of a fluorophore and the relevant assembly. Accordingly, a 1,4-bis(phenylethynyl)benzene (BPEB) derivative (**C2**) with two cholesteryl residues in the side chains and two glucono units in the head and tail positions was designed and synthesized. As a control, compound **C1** was also prepared. The only difference between **C1** and **C2** is that the hydroxyl groups in the glucono residues of **C1** are fully acetylated. Studies of the fluorescence behaviors of the two compounds in solution revealed that both the profile and the intensity of the fluorescence emission of the compounds, in particular **C2**, are dependent on their concentration and on the nature of solvents employed. Presence of HCl also alters the emission of the compounds in solution. On the basis of the studies, three fluorescent films were prepared, and their sensing performances to HCl in vapor state were studied. Specifically, Film 1 and Film 3 were fabricated via physical coating, separately, of **C2** and **C1** on glass plate surfaces. As another comparison, Film 2 was also fabricated with **C2** as a fluorophore but at a much lower concentration if compared to that for the preparation of Film 1. As revealed by SEM and fluorescent microscopy studies, Film 1 and Film 2 exhibit well-defined microstructures, which are spherical particles and spherical pores, respectively, while Film 3 is characterized by irregular aggregates of **C1**. Fluorescence measurements demonstrated that Film 1 and Film 3 both display an aggregation emission, of which the emission from Film 1 is supersensitive to the presence of HCl vapor (detection limit: 0.4 ppb, a lowest value reported in the literatures). For Film 3, however, its emission is insensitive to the presence of the vapor. Similarly, the emission from the nonaggregated state of **C2**, a characteristic emission of Film 2, is also insensitive to the presence of the vapor. Furthermore, the sensing process of Film 1 to the vapor is highly selective and fully reversible, which lays foundation for its real-life uses. As for **C2**, the results from solution studies and those from film studies demonstrate clearly that introduction of auxiliary structures with opposite properties onto a typical fluorophore is a good strategy to develop fluorescent supramolecular motifs with rich assembly properties and great potential of applications.

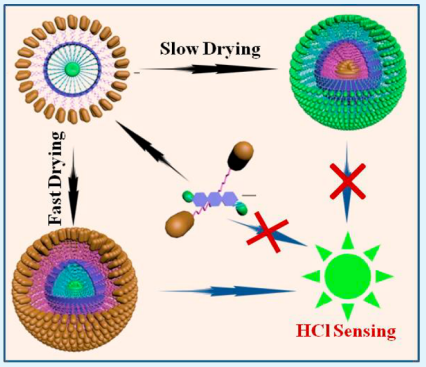

KEYWORDS: *glucose, cholesterol, fluorescence, 1,4-bis(phenylethynyl)benzene (BPEB), self-assembly*

INTRODUCTION

Hydrochloric acid (HCl) is listed as a Title III hazardous air pollutant since it is not only detrimental to the environment,[1−3] but also one of the most commonly used acids in industry and the most intense gas emitted from various sources.[4,5] Therefore, development of sensitive and reliable HCl sensors has been a matter of great concern during the past few years. Itagaki and co-workers reported a fiber-optical HCl sensor based on porphyrin-dispersed composites and various polymer matrices, which allows the HCl vapor detectable at the concentrations greater than 0.8 ppm.[6] Very recently, Matsuguchi and colleagues developed a mass type HCl sensor by coating specially prepared poly(*N*-isopropylacrylamide) nanoparticles onto the quartz resonator of a quartz crystal microbalance (QCM) and detection of ppm level of HCl was realized by using the technique.[7] However, the sensitivities of the methods as developed cannot meet the requirement of relevant regulations.[8] In the face of this challenge, amperometric,[9] conductometric,[10] and solid electrochemical methods[11] were also developed for the measurements. Moreover, the methods as mentioned also suffered from some drawbacks, for example, troublesome, time-consuming and difficult to be developed into devices.

Compared to the mass-type and electrochemical techniques, fluorescence methods possess a number of advantages such as great sensitivity, high selectivity, reference-free, and abundant signals, etc.[12−14] In particular, film-based fluorescent sensors are reusable and almost no contamination to the samples under study.[15] In a previous study, our group reported a fluorescent HCl film sensor based on a specially designed co-oligomer,

Received: August 19, 2014
Accepted: October 14, 2014
Published: October 14, 2014

which had been prepared by condensation of ethanediamine with a 1,4-bis- (phenylethynyl)benzene (BPEB) derivative.[16] The fluorescence emission of the film is sensitive and selective to the presence of HCl vapor, but the reversibility is not as good as required. Accordingly, more fluorescent films with superior performances to the sensing of HCl are still need to be developed.

It is known that there are a number of factors affecting the sensing performances of a fluorescent film, for example, the nature of the fluorophor, the substrate adopted, and the ways utilized for the fabrication of the films. Among them, the internal structure of the adlayer of the fluorophore plays a critical rule for the performances of the films,[17−19] of which the porosity, the permeability, and the thickness of the adlayer are the key factors to determine the speed, the selectivity and the sensitivity of the film sensors. Therefore, controllable fabrication of the films with designed adlayer structure is of great importance. Accordingly, no doubt the creation of fluorophores with required structures and selection of fabrication methods for the immobilization of the fluorophores on a substrate surface are two main ways to control the structures.

Self-assembly is one of the most important concepts commonly used in scientific field in the 21st century. It is defined as the process by which a system's components arrange into defined architectures[20] via noncovalent interactions, such as hydrogen bonding, dipole−dipole interaction, van der Waals interaction, $\pi-\pi$ interaction, metal−ligand coordination, hydrophobic and hydrophilic interaction, or a combination of several of them.[21−25] BPEB, because of its conjugated structure, possesses the so-called molecular wire or superquenching effect[26−28] and has been widely used in fluorescent sensing.[29−32] Cholesterol is a natural compound, and is a commonly used unit for creation of supramolecular building blocks due to its rigid skeleton, several sterogenic centers, and the strong tendency to form aggregates via van der Waals interactions.[33,34] Meanwhile, glucose is a polyhydroxy compound, and possesses the ability to form multiple intermolecular and intramolecular hydrogen bonds,[35] which lays foundation for derivatizing into different structures.[36−38]

It is well-known that most of the fluorophores show monomolecular emission at low concentrations, while increasing concentration leads to aggregate emission. As an example, pyrene and its derivatives, the widely used fluorescent probes, exhibit two distinct emission bands at moderately concentrated solutions, fine structured band around 390 nm and broad structureless band around 490 nm, namely, the monomer emission and the excimer emission, respectively.[18,39] For sensing, differential monomer and excimer quenching have been reported,[40] and furthermore, for the systems with both monomer and excimer emissions, the sensors only depending upon one of the emissions were also reported.[41] Accordingly, it is reasonable to anticipate that other fluorophors, such as BPEB, might also exhibit this kind of aggregate related sensing distinction.

Upon the basis of the afore-described idea, a molecule (**C2**) with cholesterol and glucose as main components was specially designed and synthesized. Figure 1 depicts the detailed structure of **C2** and a reference compound **C1**, of which the only difference between them is that for **C1** the hydroxyl groups are fully acetylated. The synthesis route is schematically shown in Supporting Information Scheme S1, and the experimental details are provided in Supporting Information.

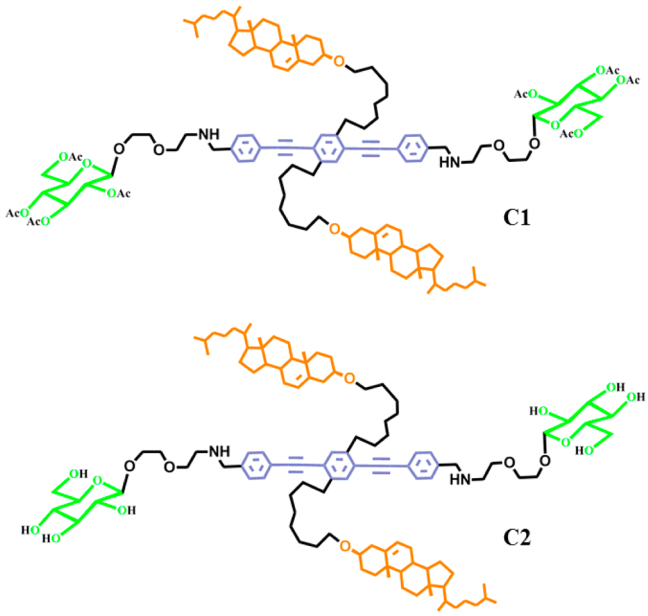

Figure 1. Molecular structure of compound **C1** and **C2**.

In the design, 1,8-dibromooctane and 2-(2-amino- ethoxy)-ethanol were employed to help the introduction of a hydrophobic structure, cholesterol and a hydrophilic structure, glucose, respectively. Furthermore, the secondary amine structure in the final compound was designed for the binding of HCl. BPEB, the core structure of **C2**, is fluorescence active, and the so-called reporting unit. Cholesterol and glucose, incompatible in property, were taken as auxiliary units and affixed in a specific manner. It was expected that with this design, a very tricky "Yin and Yang", in Chinese philosophy, balance would be established, which must be helpful for formation of ordered aggregates or supramolecular structures in solution state, a basis for smart sensing. This paper reports the details.

EXPERIMENT SECTION

Materials. β-D-Glucose pentaacetate (Alfa, >98%), trimethylsilyl trifluoromethanesulfonate (TCI, >98%), 2-(2-aminoethoxy)ethanol (TCI, >98%) and trichloroacetonitrile (TCI, >98%) were used as received. All manipulations for the preparation of the samples were performed using standard vacuum line and Schlenk technique under a purified argon atmosphere. DMF and dichloromethane were distilled from calcium hydride under argon prior to use. Methanol was distilled from magnesium under argon before use. All other reagents were of analytical grade and used without further purification or treatment. Water used in this work was acquired from a Milli-Q reference system.

Measurements. ^{1}H NMR spectra were acquired on Bruker AV 400 NMR spectrometer. Pressed KBr disks for the powder samples were used for the transmission infrared (FTIR) spectroscopy measurements, and their FTIR spectra were measured on a Fourier Transform Infrared Spectrometer. The MS were collected on a Bruker maxis UHR-TOF mass spectrometer in ESI positive mode. Melting point measurement was conducted on X-5 Microscopic melting point meter (Beijing Tech Instrument). SEM pictures of the films were acquired on a Quanta 200 scanning electron microscope (Philips-FEI). Optical and fluorescence microscopic observations were carried out on a Nikon ECLIPSE Ti−U (Nikon, Japan). TEM image was obtained using JEOL JEM-2100 transmission electron microscope at an acceleration voltage of 200 kV. DLS measurement was conducted on a Malvern Zeta Sizer Nano-ZS90. Fluorescence measurements were performed at room temperature on a time-correlated single photon counting Edinburgh Instruments FLS 920 fluorescence spectrometer

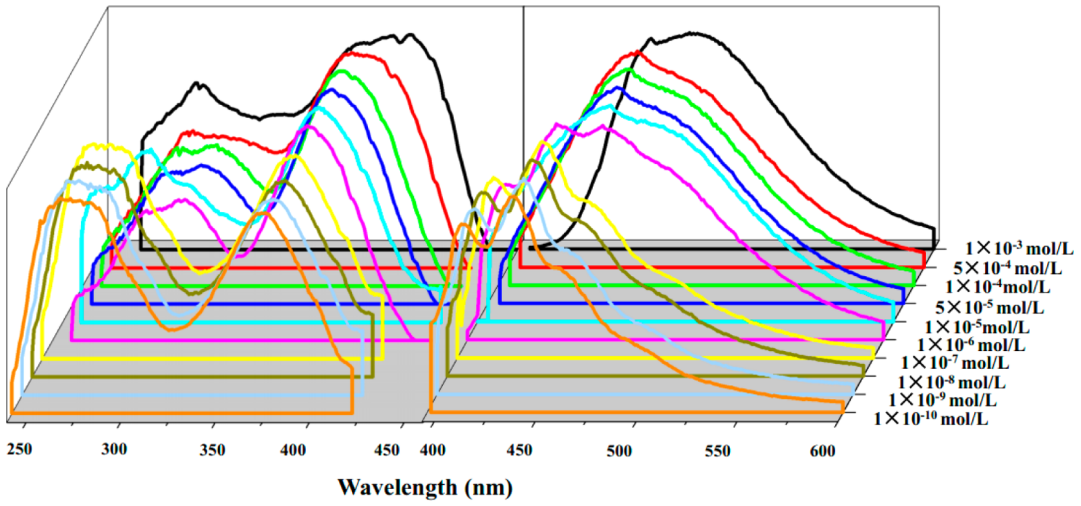

Figure 2. Fluorescence excitation and emission spectra of **C2** recorded in chloroform solution at different concentrations.

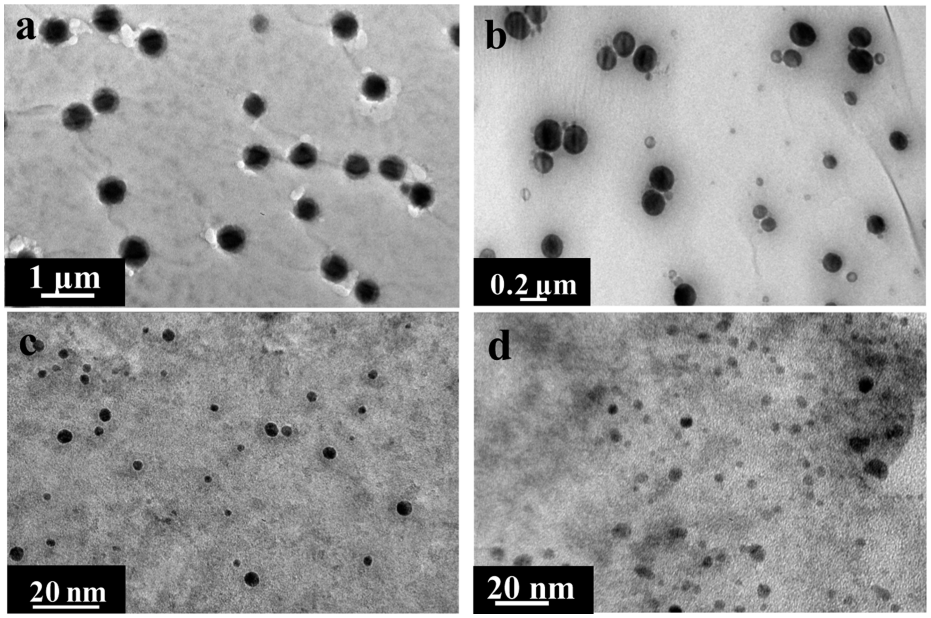

Figure 3. TEM images of **C2**: (a) 1.0×10^{-3} mol/L, chloroform solution, (b) 1.0×10^{-4} mol/L, chloroform solution, (c) 1.0×10^{-5} mol/L, chloroform solution, and (d) 1.0×10^{-5} mol/L, aqueous solution.

with a front-face method. For solvent effect studies, however, the measurements were conducted in a right-angle geometric way.

Fabrication of the Films. To fabricate Film 1, a solution of **C2** (1×10^{-3} mol/L) in chloroform was prepared. The silica substrates (0.9 cm × 2.5 cm) were cleaned by immersion in chromic acid solution for at least 3 days, and then rinsed thoroughly with plenty of water. Finally, the wet substrate was dried at 100 °C in a dust-free oven for 1 h. A defined amount (30 μL) of the **C2** solution as prepared was added onto the surface of the prepared silica plate under moist air (relative humidity of about 75%) at the ambient temperature. The high relative humidity was achieved by taking advantage of saturated sodium chloride solution. After the solvent was completely evaporated, the film was acquired.

The reference films were fabricated using the same method mentioned above; when the chloroform solution of **C2** with a concentration of 1×10^{-4} mol/L was used, Film 2 was fabricated. When the chloroform solution of **C1** with a concentration of 1×10^{-3} mol/L was used, Film 3 was fabricated.

RESULTS AND DISCUSSION

Optical Behavior of C2 in Solution State. *Concentration Effect.* From the structure of **C2**, it is reasonable to anticipate that the profile of its fluorescence spectra is concentration dependent when a definite solvent is chosen. To figure out the exact effect, the fluorescence emission and excitation spectra of a series of solutions of **C2** in chloroform were measured. It was found that with progressive increase of the concentration, the intensities of both emission and excitation increase dramatically. However, the most pronounced change is in the profile and position of the excitation and the emission. To be clear, Figure 2 shows the normalized spectra taken at different concentrations of the compound. With reference to the figure, it is seen that the maximum excitation for solutions with concentrations from 1×10^{-10} to 1×10^{-5} mol/L appears around 370 nm. However, a noticeable progressive red shift takes place for solutions of concentrations from 5×10^{-5} to 1×10^{-3} mol/L, which may be taken as a

dx.doi.org/10.1021/am505588x | ACS Appl. Mater. Interfaces 2014, 6, 20016−20024

result of the formation of aggregates of the compound, BPEB. Furthermore, there are also some changes appeared below 350 nm in the excitation spectra of the systems.

As for the fluorescence emission, those with concentrations within 1×10^{-10} and 1×10^{-8} mol/L are characterized by four peaks, centering at 410, 440, 460, and 500 nm, respectively. For solution with a concentration of 1×10^{-7} or 1×10^{-6} mol/L, the four peaks are still there, but the first decreases and the last increases along with increasing the concentration of the compound. Along with the change described, a more pronounced variation is the red shift of the longer wavelength side of the emission. Further increasing the concentration of the compound resulted in a broad and structureless emission around 480 nm, a clear indication of aggregate emission. This kind of spectra changes may be attributed to the lattice softening effect as proposed by Yao and co-workers in the studies of emission from fluorescent nanoparticles.[42] In the studies, the authors found that the particles' emission shifted to longer wavelengths along with increasing their sizes. To confirm the explanation, the aggregation of **C2** in chloroform was examined via TEM measurements. For the solution of 1×10^{-4} mol/L, it was found that **C2** self-assembled into spherical aggregates varying from 100 to 200 nm as shown in Figure 3b. This result was further confirmed by the results from Dynamic Light Scattering (DLS) studies (Supporting Information Figure S1). For the solutions of 1×10^{-3} and 1×10^{-5} mol/L, the average diameters of the spherical aggregates are 700 and 10 nm, respectively (Figure 3a,c). The big differences of the particle sizes may explain why the emission shifted to longer wavelengths with increasing the concentrations in the solvent. With further examination of the emissions shown in Figure 2, it is easy to find out that the compound aggregates even at a concentration of 1×10^{-7} mol/L. Considering the fact that chloroform is a good solvent for BPEB and the cholesteryl units of **C2**, the key structures of the compound, and a poor solvent for glucono unit, it should be reasonable to infer that the aggregation mainly originated from the association of the glucose moieties of different **C2** molecules. It is this association that narrows the distance of the fluorescent BPEBs and this may explain why the compound aggregates at so low concentrations. An opposite phenomenon can be found in aqueous phase due to aggregation of the cholesteryl structure and the BPEB unit as evidenced by the result from TEM observation (Figure 3d) and the fluorescence measurements (cf. Figure 4 and discussion below).

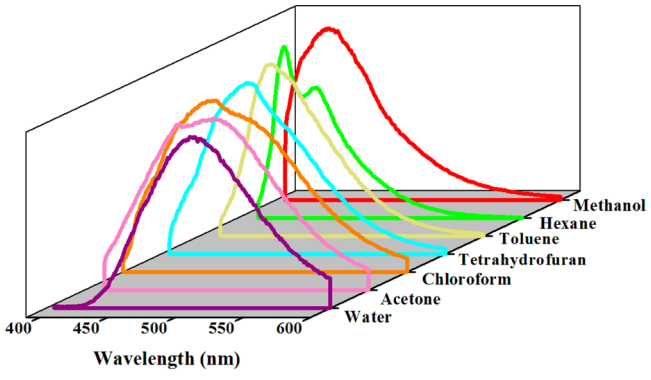

Figure 4. Fluorescence emission spectra of **C2** recorded in its solutions of different solvents at a concentration of 1×10^{-5} mol/L (λ_{ex} = 370 nm).

Solvent Effect. Fluorescence measurement was conducted in a variety of solvents including methanol, hexane, toluene, THF, chloroform, acetone, and water, of which the polarity is different from each other, at the concentration is 1×10^{-5} mol/L. It has been shown that the intensity, the profile, and the position of the fluorescence emissions of the compound change along with variation of the solvent. As shown in Figure 4, the maximum emission of the methanol solution appears around 430 nm, and the others at 424, 442, 450, 460, 480, and 500 nm, respectively. No typical monomolecular emission as shown in Figure 2 for the solutions of concentrations higher than 1×10^{-8} mol/L suggests that the compound may stay in aggregated state in all the samples under study. This is not difficult to understand due to neither nonpolar solvent nor polar solvent are fully compatible to all the building components of **C2**, and the concentration of the compound is relatively high. Further examination of the spectra reveals that there are big differences in the profiles of the emissions, indicating the complexity of the structures of the aggregates. Considering the results shown in Figure 2 and those shown in Figure 4, it may not be difficult to infer that the emission may originate from three states of the compound in the solutions, of which one is the monomolecular state of BPEB component, the partially overlapped state, and the fully overlapped state. As shown in Figures 2 and 4, the emissions from the three states are characterized by the emissions appearing at or around 420, 460, and 500 nm, respectively. Clearly, for the compound in chloroform, the emissions are mainly coming from the monomolecular state when its concentration is equal or lower than 1×10^{-8} mol/L. Carefully inspection of the emission spectra shown in Figure 2 clearly shows that within the concentration range concerned, the contribution from partially overlapped state increases along with increasing the concentration of the compound. With further increase of the concentration of the compound, the profile of the emission changes significantly and shifts to longer wavelengths. It is not difficult to find that further increase of the concentration makes the contribution from the fully overlapped state increase, and eventually dominated by it when the concentration exceeds 1×10^{-5} mol/L.

As discussed already, the emission of the compound, at least for solutions of a concentration of 1×10^{-5} mol/L, is highly dependent on the nature of its medium (cf. Figure 4). Specifically, the emission from methanol solution contains contributions from the monomolecular state and the partially overlapped state. However, the emission from aqueous solution is almost a pure emission of the fully overlapped state. As for the others, they are mixtures of the emissions from different overlapped states. It is to be noted that for all the emissions shown in Figure 4 except the two from methanol and hexane, there is almost no contribution from the monomolecular state. These findings reveal that the compound as prepared possesses a strong tendency to form various aggregates either in nonpolar solvents or polar solvents. This is not difficult to understand due to the specific structure of the compound. As it is seen that the core structure of the compound is BPEB, containing three benzene rings, this makes it possible to form different overlap structures which may be two over two benzene rings, and three over three, respectively. It is this multiple overlap possibility and the amphiphilic property of the compound that makes the molecules of the compound adopt abundant conformations and/or different aggregate structures. This may explain why **C2** shows so colorful fluorescence behavior in different solvents and at different concentrations.

Fluorescence measurement of **C2** was also conducted at a concentration of 1×10^{-8} mol/L with all the solvents mentioned above. The results are shown in Supporting Information Figure S2. It is seen that the profiles and the positions of the emissions from this concentration are very different from those of the emission spectra recorded at the concentration of 1×10^{-5} mol/L, suggesting appearance of the monomolecular state of the compound in the solutions under study except aqueous solution.

Solid-State Fluorescence in Film State. *Characterization of Films.* The excitation and emission spectra of the fluorescent films as prepared were measured and the results are depicted in Figure 5. It can be seen that the maximum excitation of Film 1 and Film 3 both appear at 370 nm, and the maximum emission at 500 nm. The emission shifts to 460 nm, while the excitation shows no significant change when Film 2 is measured. To understand the change in fluorescence emission, the microstructures of the adlayers of the films were investigated. Figure 6 shows the fluorescence microscope image (Figure 6a) and the SEM image (Figure 6b) of Film 1. Reference to the images revealed that **C2** aggregated into well-defined spherical particles of diameters between 1 and 3 μm. For Film 2, spherical pores with an average diameter of 10 μm were found on the film (cf. Supporting Information Figure S3a,b). For Film 3, however, it does not possess well-defined structure, a property very different from that of Film 1 (cf. Supporting Information Figure S3c,d). The irregular characteristic of the adlayer structure of Film 3 may be attributed to the lack of amphiphilic structure of **C1**, which was used for the fabrication of the film. The distinction of the microstructures might explain the difference between the emissions and excitations of the three films (cf. Figure 5). It is to be noted that the films as fabricated are photochemically stable, which is a prerequirement for further application studies.

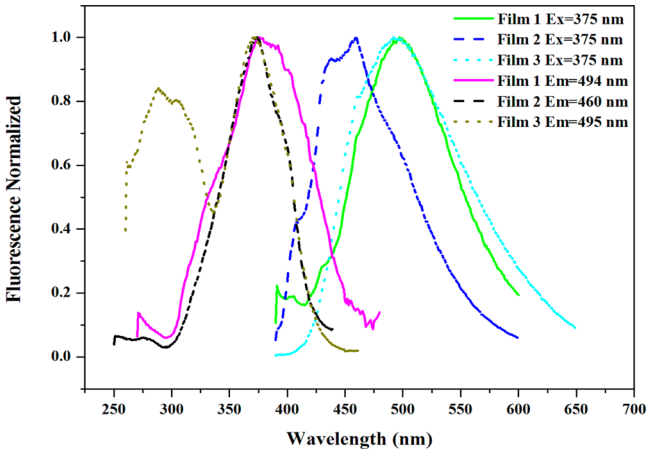

Figure 5. Excitation and emission spectra of Film 1, Film 2, and Film 3 in dry state.

Sensing Performance Studies. The sensing response of Film 1 to HCl vapor was intensively studied by measuring the fluorescence variation in the presence of various concentrations of HCl vapor. The fluorescence tests were conducted in the following way: first, a film to be tested was adhered to one side of a quartz cell and the fluorescence emission spectrum of the film was recorded, and then put the cell into a chamber with specific concentration of HCl vapor. Five minutes later, the fluorescence spectrum of the film was recorded again. Figure 7 depicts the fluorescent spectra and the Stern–Volmer plot of the measurements. It is found that a trace amount of HCl vapor, as low as 4 ppb, can cause noteworthy fluorescent quenching (25%). When the concentration increased to 48 ppb, no further quenching was detected, indicating the

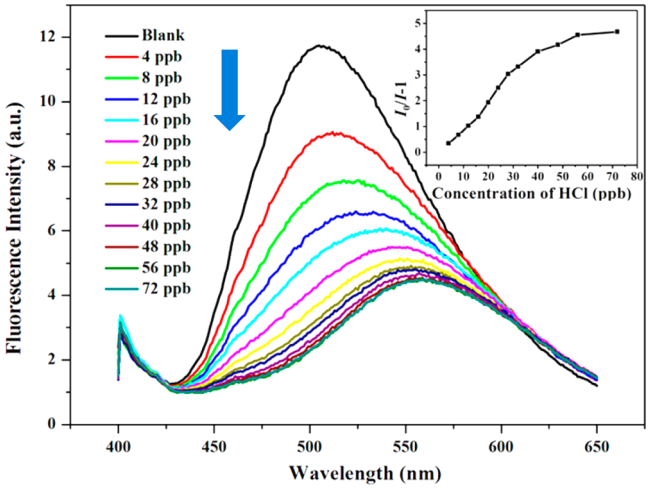

Figure 7. Fluorescence emission spectra and Stern–Volmer plot (inset) of Film 1 in the presence of different concentrations of HCl (data error: ±3%).

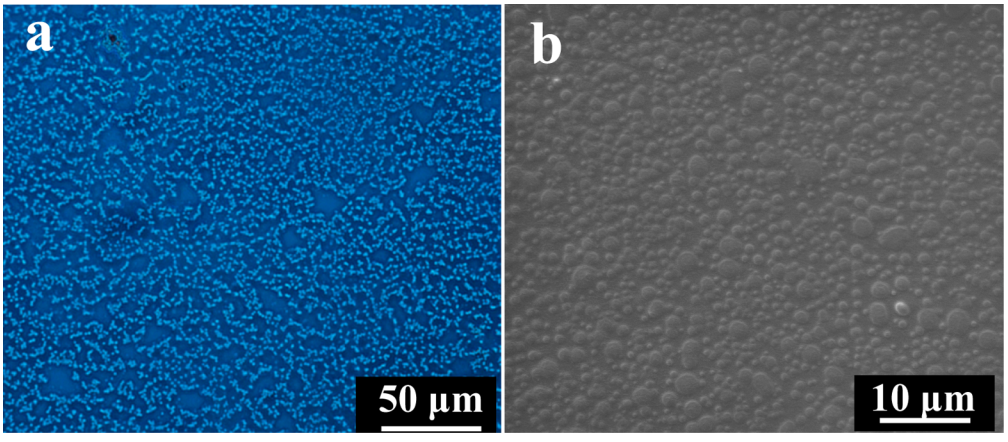

Figure 6. Fluorescent micrograph (a) and SEM image (b) of Film 1.

uttermost decrease of fluorescence intensity. To our knowledge, this is the most sensitive film for HCl vapor detection since its detection limit (DL) reaches 0.4 ppb, a lowest value reported in the literatures. The details of the DL calculation are provided in the Supporting Information. On the other side, it can be seen from the Stern−Volmer plot that the fluorescence quenching of the film is close to linear at concentrations lower than 30 ppb, but derives from the linearity at higher concentrations.

As a comparison, the sensing performance to HCl vapor of Film 2, of which the only difference with Film 1 is that the solution of **C2** used for the fabrication is 10 times lower than that used for the preparation of Film 1, is also investigated and the results are shown in Supporting Information Figure S4. Unfortunately, HCl vapor of ppb level shows no effect to the fluorescence emission of the film, and a concentration nearly 100 ppm of HCl vapor could cause an obvious quenching. In addition, greatly increasing HCl concentration, from 88 to 2860 ppm, resulted in only 25% decrease of the emission.

As another control, the sensing performance of Film 3 was also studied. In this case (cf. Supporting Information Figure S5), it is seen that the sensitivity fell to 176 ppb. In other words, this is a concentration needed to induce an evident fluorescence quenching. Meanwhile, addition of 2 ppm of HCl vapor resulted in less than 60% reduction of the initial emission of the film.

The quenching results from comparative studies as described indicate that the sensing performance of the films is not only determined by the nature of the sensing fluorophore as evidenced by the difference in the sensing performance of Film 3 to that of Film 1 and Film 2, but also determined by the structures of the aggregates, as evidenced by the big difference in the sensing performances of Film 1 and Film 2, a result in support of the statement that functional materials could be created by either chemical synthesis or physical assembly. As for why Film 1 is much more sensitive to the presence of HCl than Film 3, it may be understood by considering the difference in the molecular structures of the fluorophores employed for fabricating the films. The glucono unit of **C2**, which was used for fabricating Film 1, can be functioning as a guide for binding HCl onto fluorescent adlayer of the film due to its hydrophilic nature, whereas **C1**, a fluorophore used for preparing Film 3, does not possess this property, and this is unfavorable for the binding of HCl, a prerequirement for sensing. This may explain why Film 1 possesses superior sensing performances to HCl.

As for **C2**, the results from solution studies and those from film studies demonstrate clearly that introduction of auxiliary structures with opposite properties onto a typical fluorophore is a good strategy to develop fluorescent supramolecular motifs with rich assembly properties and great potential of applications.

The response speed of Film 1 to HCl vapor was investigated by monitoring its fluorescence intensity as a function of time at a definite concentration of the analyte. Specifically, a concentration of 48 ppb HCl was employed to conduct the test, and fluorescence emission spectrum was recorded for every definite quenching time. The results are shown in Supporting Information Figure S6. It is seen that the fluorescence quenching by HCl vapor is fast and 5 min are enough for the quenching to reach equilibrium.

Selectivity is a vital factor to determine the real-life application of sensing films. Accordingly, influence of other acidic vapors, such as formic acid, nitric acid, acetic acid, hydrofluoric acid, hydroiodic acid, hydrobromic acid, sulfuric acid, phosphoric acid, as well as common solvents in vapor phase, including phenol, aniline, toluene, benzene, water, chloroform, acetone, THF and methanol, on the fluorescent emission was studied, and the results are shown in Supporting Information Figure S7. Reference to the figure reveals that the intensity of the fluorescence emission changed a little except formic acid and nitric acid show some interference when it was exposed to 66 ppm of the interferents mentioned above while 48 ppb of the HCl vapor, only 1/1000 of the concentrations of the interferents, causes 80% decrease of the initial emission of the film. As for the understanding of the selectivity of Film 1 to the sensing of HCl to other acids in vapor phase, the reasons behind might be very complicated. However, the most important factors affecting the sensing might be the strength of the acids and their sizes. For the acids tested, the size of HCl is significantly smaller than HBr, HI and the oxoacids tested, and at the same time its acidity is much stronger than that of HF, and this may explain why HCl shows much higher quenching efficiency to the fluorescence emission of the film.

Reversibility is another important factor which must be highly concerned if the film is expected to be used practically. The procedures adopted for the examination of the reversibility of the sensing process are as follows: The film was first inserted into a cell, the fluorescence emission was measured as blank, and then, the film was exposed to a definite concentration of HCl vapor for 5 min and the fluorescent emission was measured again. After the measurement, the fluorescence intensity of the film was recovered by exposure to saturated ammonia vapor for 10 s. The whole process was repeated eight times using different concentrations of HCl vapor. It is clearly manifested in Figure 8 that the response of Film 1 to HCl vapor is fully reversible, good news for practical uses.

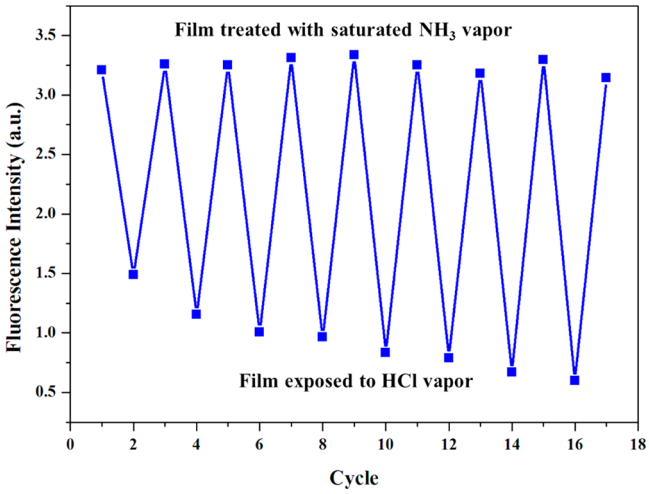

Figure 8. Reversibility of the response of Film 1 to HCl vapor at different concentrations (from left to right: 44, 88, 880, 15, 154, 616, 1540 ppm and saturated vapor).

Quenching Mechanism. To understand the mechanism of the quenching process, fluorescence lifetime measurements were conducted, and the results from the measurements were made comparison with those from static measurements. As shown in Supporting Information Figure S8, the intensity based Stern−Volmer plot shows a downward curvature, while the lifetime-based plot is almost a straight line with a slop of nearly

zero, suggesting that the quenching is dominated by formation of a non/weak-fluorescent complex, **C2**−HCl, a typical static quenching process.

To identify the formation of the ground-state complex, ^{1}H NMR titration was carried out, supposing the interaction between C6 and HCl vapor may result in significant changes in the chemical shifts of the relevant protons in C6. Supporting Information Figure S9 shows that the protons of the secondary amine group disappear with the ratio of C6 to HCl increased from 1:0 to 1:1 in mole to mole. In addition, the variation of the chemical shifts of the protons besides secondary amine group and in BPEB is further evidence to support the interaction between HCl and the secondary amine group of **C2**. The sensing mechanism proposed may also apply to **C1** based films even though their performances are different.

To further understand the mechanism of the sensing process, fluorescence quenching studies of **C2** in solution state with different concentrations were conducted. The results are depicted in Supporting Information Figure S10. Concentrations of 1×10^{-4} and 1×10^{-8} mol/L of the compound in chloroform were chosen since it is believed that in the lower concentration the compound exists mainly in monomolecular state, but in the higher concentration, it exists in aggregated state as can be seen from the initial profiles and positions of the two solutions shown in Supporting Information Figure S10. With reference to the figures, it may be safe to say that in solution state, generally speaking, HCl is not a very efficient quencher of the fluorescence emission of the compound. In addition, comparison of the results shown in the figures demonstrates that the monomer emission of the compound is more sensitive to the presence of HCl than the emission from the aggregated state. This is a result contrary to that observed in the sensing performance studies of the films, which might be understood by considering the difference in the microenvironment experienced by the compound in solution state and solid state. This tentative explanation is supported by the results from contact angle (CA) measurements of the films under different conditions as shown in Supporting Information Figure S11. With reference to the figures, the contact angle of Film 1 decreased from 44.8 ± 0.6° to 31.5 ± 1.2° compared to the clean silica substrates, indicating the glucose moieties were exposed on the surface of the substrate. This is not a surprising result considering that the glucono moieties of the compound should be buried with the aggregates when it is dissolved in chloroform due to their hydrophilicity, but for the films, the situation must be different since the hydrophilic nature of the glass substrate surface and high relative humid atmosphere may reverse the structure of the aggregates in solution state. It is no doubt that exposing of the glucono units must favor the protonation of the secondary amine groups of the compound, which is essential for the quenching. This may explain why in solution state, where a nonpolar liquid was used as a solvent, the emission from the monomolecular state is more sensitive to the presence of the acid, and also why in film state, the emission from the aggregated state is more sensitive to the acid vapor.

The explanation described above is further supported by the result from an additional experiment. In the experiment, the solution used to fabricate Film 1 was added onto a hot glass substrate surface. It was believed that this would make the solvent of the solution evaporate instantly, and thereby blocks the inversion of the structure of the aggregates. Actually, the contact angle of the film prepared in this way increased to 86.7 ± 2.3°, confirming the argument as described (cf. Supporting Information Figure S11). For clarity, the structures of the aggregates of **C2** in different situations as discussed are schematically shown in a cartoon (cf. Scheme 1).

Scheme 1. A Cartoon Shows Possible Structures and Responses to HCl of a Derivative of 1,4-Bis(phenylethynyl)benzene (BPEB) (C2) and Its Aggregates in Different Mediums and on the Films Dried with Different Methods

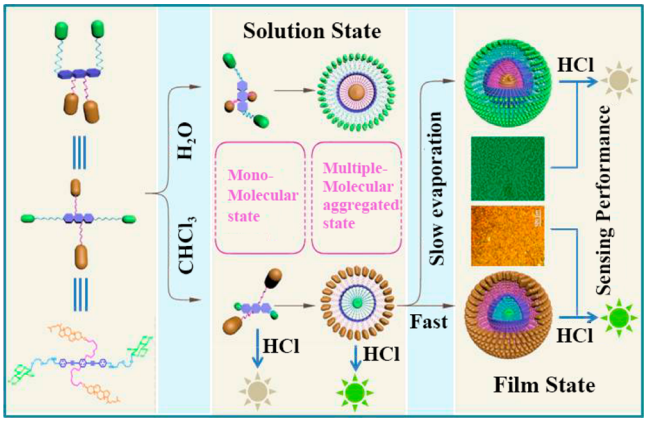

CONCLUSIONS

In conclusion, in the light of balance between "Yin and Yang", an idea from Chinese philosophy, a novel BPEB derivative was designed and prepared via simultaneous introduction of hydrophobic cholesteryl units and hydrophilic glucono structures into its side positions and the two ends. Solution behavior studies revealed that the emission of the compound could originate from the monomolecular state, the partially overlapped state, and the fully overlapped state or a combination of them, which makes the profile of the emission be highly dependent upon the solvent nature and the concentration of the compound under study. On the basis of solution behavior studies, the compound was used for fabricating fluorescence films, and it was found that the film, of which the adlayer is mainly composed of spherical aggregates, is more sensitive to the presence of HCl vapor with a DL of 0.4 ppb, a lowest value reported in the literatures until now. Furthermore, the sensing process is fully reversible, and presence of 1000 times more of other commonly found acids or organic liquids, excepting formic acid and nitric acid, shows little effect to the fluorescence emission of the film. Mechanism studies demonstrated that the nature of the quenching process is the formation of a non- or weak fluorescent complex that is the protonated **C2**.

ASSOCIATED CONTENT

Supporting Information

Detailed experimental methods, determination of detection limit and supplementary figures and schemes. This material is available free of charge via the Internet at http://pubs.acs.org.

AUTHOR INFORMATION

Corresponding Author

*E-mail: yfang@snnu.edu.cn.

Notes

The authors declare no competing financial interest.

"Yin and Yang" philosophy is a duality thinking bearing some resemblance to the dialectical thinking in the West encouraging us to embrace the opposite aspects within one object, and it also means that to achieve harmony, there must be a balance between "Yin and Yang".

■ ACKNOWLEDGMENTS

This work was supported by the Natural Science Foundation of China (21206089, 21273141), the "111 Project", and the "Program for Changjiang Scholars and Innovative Research Team in University" of China (IRT1070). We gratefully acknowledge the assistance of Professor Kevin D. Belfield (University of Central Florida) for his inspirational discussions on understanding the quenching mechanism.

■ REFERENCES

(1) Misra, S. C. K.; Mathur, P.; Yadav, M.; Tiwari, M. K.; Garg, S. C.; Tripathi, P. Preparation and Characterization of Vacuum Deposited Semiconducting Nanocrystalline Polymeric Thin Film Sensors for Detection of HCl. *Polymer* **2004**, *45*, 8623−8628.

(2) Supriyatno, H.; Yamashita, M.; Nakagawa, K.; Sadaoka, Y. Optochemical Sensor for HCl Gas Based on Tetraphenylporphyrin Dispersed in Styrene-Acrylate Copolymers. *Sens. Actuators, B* **2002**, *85*, 197−204.

(3) Jeon, H.; Lee, J.; Kim, M. H.; Yoon, J. Polydiacetylene-based Electrospun Fibers for Detection of HCl Gas. *Macromol. Rapid Commun.* **2012**, *33*, 972−976.

(4) Matsuguchi, M.; Kadowaki, Y.; Noda, K.; Naganawa, R. HCl Gas Monitoring based on a QCM Using Morpholine-Functional Styrene-co-chloromethylstyrene Copolymer Coatings. *Sens. Actuators, B* **2007**, *120*, 462−466.

(5) Wang, X. F.; Wang, J. L.; Si, Y.; Ding, B.; Yu, J. Y.; Sun, G.; Luo, W. J.; Zheng, G. Nanofiber-Net-Binary Structured Membranes for Highly Sensitive Detection of Trace HCl Gas. *Nanoscale* **2012**, *4*, 7585−7592.

(6) Itagaki, Y.; Yamanaka, S.; Sadaoka, Y. HCl Detection using Polymer-Porphyrin Composite Coated Optical Fiber Sensor. *Sens. Lett.* **2011**, *9*, 114−117.

(7) Matsuguchi, M.; Harada, N.; Omori, S. Poly(N-isopropylacrylamide) Nanoparticles for QCM-Based Gas Sensing of HCl. *Sens. Actuators B* **2014**, *190*, 446−450.

(8) Occupational Safety and Health Administration (OSHA). *Occupational Safety and Health Standards, Toxic and Hazardous Substances*. Code of Federal Regulations. 29 CFR 1910.1000. 1998.

(9) Imaya, H.; Ishiji, T.; Takahashi, K. Detection Properties of Electrochemical Acidic Gas Sensors Using Halide-Halate Electrolytic Solutions. *Sens. Actuators, B* **2005**, *108*, 803−807.

(10) Bavastrello, V.; Stura, E.; Carrara, S.; Erokhin, V.; Nicolini, C. Poly(2,5-dimethylaniline)-MWNTs Nanocomposite:A New Material for Conductometric Acid Vapours Sensor. *Sens. Actuators, B* **2004**, *98*, 247−253.

(11) Wang, L.; Kumar, R. V. Thick Film Miniaturized HCl Gas Sensor. *Sens. Actuators, B* **2004**, *98*, 196−203.

(12) Cui, H.; He, G.; Wang, H. Y.; Sun, X. H.; Liu, T. H.; Ding, L. P.; Fang, Y. Fabrication of a Novel Cholic Acid Modified OPE-based Fluorescent Film and Its Sensing Performances to Inorganic Acids in Acetone. *ACS Appl. Mater. Interfaces* **2012**, *4*, 6935−6941.

(13) Desmonts, L. B.; Reinhoudt, D. N.; Calama, M. C. Design of Fluorescent Materials for Chemical Sensing. *Chem. Soc. Rev.* **2007**, *36*, 993−1017.

(14) Naddo, T.; Che, Y. K.; Zhang, W.; Balakrishnan, K.; Yang, X. M.; Yen, M.; Zhao, J. C.; Moore, J. S.; Zang, L. Detection of Explosives with a Fluorescent Nanofibril Film. *J. Am. Chem. Soc.* **2007**, *129*, 6978−6979.

(15) Ji, X. F.; Yao, Y.; Li, J. Y.; Yan, X. Z.; Huang, F. H. A Supramolecular Cross-Linked Conjugated Polymer Network for Multiple Fluorescent Sensing. *J. Am. Chem. Soc.* **2013**, *135*, 74−77.

(16) Wang, H. Y.; Cui, H.; Liu, X. L.; Li, L. L.; Cao, Y.; Liu, T. H.; Fang, Y. Alternative Copolymerization of a Conjugated Segment and a Flexible Segment and Fabrication of a Fluorescent Sensing Film for HCl in the Vapor Phase. *Chem.—Asian J.* **2013**, *8*, 101−107.

(17) Peng, H. N.; Ding, L. P.; Liu, T. H.; Chen, X. L.; Li, L.; Yin, S. W.; Fang, Y. An Ultrasensitive Fluorescent Sensing Nanofilm for Organic Amines based on Cholesterol-Modified Perylene Bisimide. *Chem.—Asian J.* **2012**, *7*, 1576−1582.

(18) Beyazkilic, P.; Yildirim, A.; Bayindir, M. Formation of Pyrene Excimers in Mesoporous Ormosil Thin Films for Visual Detection of Nitro-Explosives. *ACS Appl. Mater. Interfaces* **2014**, *6*, 4997−5004.

(19) Liu, K.; Liu, T. H.; Chen, X. L.; Sun, X. H.; Fang, Y. Fluorescent Films based on Molecular-Gel Networks and Their Sensing Performances. *ACS Appl. Mater. Interfaces* **2013**, *5*, 9830−9836.

(20) Palma, C. A.; Cecchini, M.; Samorì, P. Predicting Self-Assembly: From Empirism to Determinism. *Chem. Soc. Rev.* **2012**, *41*, 3713−3730.

(21) Lackinger, M.; Griessl, S.; Markert, T.; Jamitzky, F.; Heckl, W. M. Self-Assembly of Benzene-Dicarboxylic Acid Isomers at the Liquid Solid Interface: Steric Aspects of Hydrogen Bonding. *J. Phys. Chem. B* **2004**, *108*, 13652−13655.

(22) Lei, Y.; Li, J.; Wang, Y. Y.; Gu, L.; Chang, Y. F.; Yuan, H. Y.; Xiao, D. Rapid Microwave-Assisted Green Synthesis of 3D Hierarchical Flower-Shaped $NiCo_2O_4$ Microsphere for High-Performance Supercapacitor. *ACS Appl. Mater. Interfaces* **2014**, *6*, 1773−1780.

(23) Elemans, J. A. A. W.; Lei, S. B.; Feyter, S. D. Molecular and Supramolecular Networks on Surfaces: From Two-Dimensional Crystal Engineering to Reactivity. *Angew. Chem., Int. Ed.* **2009**, *48*, 7298−7332.

(24) Surin, M.; Samorì, P.; Jouaiti, A.; Kyritsakas, N.; Hosseini, M. W. Molecular Tectonics on Surfaces: Bottom-Up Fabrication of 1D Coordination Networks that Form 1D and 2D Arrays on Graphite. *Angew. Chem., Int. Ed.* **2007**, *46*, 245−249.

(25) Isojima, T.; Suh, S. K.; Sande, J. B. V.; Hatton, T. A. Controlled Assembly of Nanoparticle Structures: Spherical and Toroidal Superlattices and Nanoparticle-Coated Polymeric Beads. *Langmuir* **2009**, *25*, 8292−8298.

(26) He, G.; Yan, N.; Kong, H. Y.; Yin, S. W.; Ding, L. P.; Qu, S. X.; Fang, Y. A New Strategy for Designing Conjugated Polymer-Based Fluorescence Sensing Films via Introduction of Conformation Controllable Side Chains. *Macromolecules* **2011**, *44*, 703−710.

(27) Albert, S. K.; Thelu, H. V. P.; Golla, M.; Krishnan, N.; Chaudhary, S.; Varghese, R. Self-Assembly of DNA-Oligo(p-phenylene-ethynylene) Hybrid Amphiphiles into Surface-Engineered Vesicles with Enhanced Emission. *Angew. Chem., Int. Ed.* **2014**, *53*, 8352−8557.

(28) Thomas, S. W.; Joly, G. D.; Swager, T. M. Chemical Sensors based on Amplifying Fluorescent Conjugated Polymers. *Chem. Rev.* **2007**, *107*, 1339−1386.

(29) Khan, A.; Müller, S.; Hecht, S. Practical Synthesis of an Amphiphilic, Non-Ionic Poly(para-phenyleneethynylene) Derivative with a Remarkable Quantum Yield in Water. *Chem. Commun.* **2005**, *5*, 584−586.

(30) Kim, I. B.; Erdogan, B.; Wilson, J. N.; Bunz, U. H. F. Sugar-Poly(para-phenylene ethynylene) Conjugates as Sensory Materials: Efficient Quenching by Hg^{2+} and Pb^{2+} Ions. *Chem.—Eur. J.* **2004**, *10*, 6247−6254.

(31) Phillips, R. L.; Kim, I. B.; Tolbert, L. M.; Bunz, U. H. F. Fluorescence Self-Quenching of a Mannosylated Poly(p-phenyleneethynylene) Induced by Concanavalin. *J. Am. Chem. Soc.* **2008**, *130*, 6952−6954.

(32) Tolosa, J.; Zucchero, A. J.; Bunz, U. H. F. Water-Soluble Cruciforms: Response to Protons and Selected Metal Ions. *J. Am. Chem. Soc.* **2008**, *130*, 6498−6506.

(33) Klok, H. A.; Hwang, J. J.; Iyer, S. N.; Stupp, S. I. Cholesteryl-(L-lactic acid) Building Blocks for Self-Assembling Biomaterials. *Macromolecules* **2002**, *35*, 746−759.

(34) Wallimann, P.; Marti, T.; Fürer, A.; Diederich, F. Steroids in Molecular Recognition. *Chem. Rev.* **1997**, *97*, 1567−1608.

(35) Altaner, C. M.; Thomas, L. H.; Fernandes, A. N.; Jarvis, M. C. How Cellulose Stretches: Synergism Between Covalent and Hydrogen Bonding. *Biomacromolecules* **2014**, *15*, 791−798.
(36) Ruppert, A. M.; Weinberg, K.; Palkovits, R. Hydrogenolysis Goes Bio: from Carbohydrates and Sugar Alcohols to Platform Chemicals. *Angew. Chem., Int. Ed.* **2012**, *51*, 2564−2601.
(37) Thomas, G. B.; Rader, L. H.; Park, J.; Abezgauz, L.; Danino, D.; DeShong, P.; English, D. S. Carbohydrate Modified Catanionic Vesicles: Probing Multivalent Binding at the Bilayer Interface. *J. Am. Chem. Soc.* **2009**, *131*, 5471−5477.
(38) Ryu, J. H.; Lee, E.; Lim, Y. B.; Lee, M. Carbohydrate-Coated Supramolecular Structures: Transformation of Nanofibers into Spherical Micelles Triggered by Guest Encapsulation. *J. Am. Chem. Soc.* **2007**, *129*, 4808−4814.
(39) Vybornyi, M.; Rudnev, A. V.; Langenegger, S. M.; Wandlowski, T.; Calzaferri, G.; Häner, R. Formation of Two-Dimensional Supramolecular Polymers by Amphiphilic Pyrene Oligomers. *Angew. Chem., Int. Ed.* **2013**, *52*, 11488−11493.
(40) Focsaneanu, K. S.; Scaiano, J. C. Potential Analytical Applications of Differential Fluorescence Quenching: Pyrene Monomer and Excimer Emissions as Sensors for Electron Deficient Molecules. *Photochem. Photobiol. Sci.* **2005**, *4*, 817−821.
(41) Morales, C. E. A.; Galian, R. E.; Prieto, J. P. Pyrene-Functionalized Nanoparticles: Two Independent Sensors, the Excimer and the Monomer. *Anal. Chem.* **2012**, *84*, 8083−8087.
(42) Xiao, D. B.; Xi, L.; Yang, W. S.; Fu, H. B.; Shuai, Z. G.; Fang, Y.; Yao, J. J. Size-Tunable Emission from 1,3-Diphenyl-5-(2-anthryl)-2-pyrazoline Nanoparticles. *J. Am. Chem. Soc.* **2003**, *125*, 6740−6745.